Polymer Bulletin (2024) 81:3333–3353
https://doi.org/10.1007/s00289-023-04873-8

ORIGINAL PAPER

Synthesis and characterization of PANI and PANI-indole copolymer and study of their antimalarial and antituberculosis activity

Purnima Chaubisa[1] · Dharmendra Dharmendra[1] · Yogeshwari Vyas[1] · Priyanka Chundawat[1] · Nirmala Kumari Jangid[2] · Chetna Ameta[1]

Received: 15 November 2022 / Revised: 31 March 2023 / Accepted: 28 May 2023 /
Published online: 6 June 2023
© The Author(s), under exclusive licence to Springer-Verlag GmbH Germany, part of Springer Nature 2023

Abstract

The preparation of polyaniline (PANI) and its copolymer with indole involved a chemical oxidative polymerization method, with benzene sulfonic acid (BSA, $C_6H_6O_3S$) used as a dopant and potassium persulfate (PPS, $K_2S_2O_8$) as an oxidant. The synthesized compounds underwent characterization using FTIR, 1H-NMR, TGA, and GPC techniques, which allowed the calculation of their average molecular weight and polydispersity index (PDI) through the GPC technique. The PDI values of the PANI copolymer with indole in different aniline-to-indole ratios were 1.53, 1.13, and 1.532 for 1:1, 1:2, and 2:1 ratios, respectively. Thermal stability was determined using TGA, revealing that the indole heterocyclic compound increased the inflexibility of the polymer chains in the synthesized PANI copolymer. The structure of the copolymer was further analyzed using ^{1}HNMR and FTIR techniques, which confirmed the existence of benzenoid and quinoid groups in the PANI-indole copolymers, as well as the effect of doping on the polymer chains. The antibacterial and antifungal properties of the copolymers were studied against several bacterial and fungal strains and measured in terms of minimum inhibitory concentration. Results indicated that the inhibition rate of the PANI-indole copolymer on *S. pyogenus* (MTCC 442) was higher than that of standard drugs and individual PANI. The PANI-indole copolymers also displayed excellent antituberculosis and antimalarial activities, with the synthesized copolymer showing better outcomes than individual PANI.

Keywords Polyaniline · BSA · Potassium persulphate (PPS) · Indole · GPC · Antimicrobial · Antimalarial · Antituberculosis activity

✉ Chetna Ameta
chetna.ameta@yahoo.com

[1] Department of Chemistry, Mohanlal Sukhadia University, Udaipur, Rajasthan, India

[2] Department of Chemistry, Banasthali Vidyapith, Banasthali, Jaipur, Rajasthan, India

Introduction

Polyaniline (PANI) is a highly researched conducting polymer with great potential for commercial applications. Over the past four decades, significant interest has been devoted to PANI, owing to its exceptional properties. However, to enhance its thermal and optical properties, researchers have explored the development of copolymers by integrating nanomaterials [1]. Nanostructured conducting polymers have emerged as promising materials in several organic electronic fields, due to their unique structural, mechanical, photoelectric, and electrical properties at the nanoscale [2].

Currently, the incorporation of nanoscale compounds is of utmost importance in various fields. Nanomaterials have found new applications in areas such as photocatalysis [3], electrochemical hydrogen storage [4, 5], recyclable degradation of organic dyes [6], efficient degradation of pollutants for environmental remediation [7], antifouling properties [8], capping agents [9], visible-light-responsive photocatalysts [10], photodecomposition [11], and drug delivery [12, 13], among others.

The unique physical, electrical, chemical, and electrochemical properties [14] of nanomaterials have generated considerable interest in the scientific community, owing to their potential for various applications. These include biosensors [15, 16], rechargeable batteries [17–19], light-emitting diodes [20, 21], electrochromic display devices [22, 23], data storage devices, transistors [24], electromagnetic intervention shielding [25], chemical sensors [26], tissue engineering, biomedicine [27], and many more. Additionally, nanomaterials possess properties such as high chemical strength, electron affinity, biocompatibility, and low toxicity, and are readily available at a low cost, making them an attractive option for a wide range of applications. [28]

The properties of conductive polymers are influenced by several factors, including the type of dopant and solvent, dopant ion size, protonation level, and preparation conditions. Altering these parameters can lead to significant changes in the electrical, optical, and structural properties of conductive polymers. The preparation of polyanilines involves the use of different acids as dopants, including both organic and inorganic acids. Electrochemical and chemical oxidative polymerization methods are commonly used for synthesizing polyanilines in an acidic medium. The electrochemical method is preferred for small-scale synthesis, while the chemical oxidative method is used for large-scale synthesis. Typically, potassium persulfate ($K_2S_2O_8$) and ammonium persulfate ($(NH_4)_2S_2O_8$) are used as oxidants for the chemical polymerization of aniline monomer [29]. This method allows for the production of conducting polymers in a dry form suitable for commercial applications.

Polyaniline (PANI) displays varying solubility in different organic solvents. Generally, a doped form of PANI is insoluble in *N*-methyl-2-pyrrolidone (NMP), dimethyl sulfoxide (DMSO), and dimethylformamide (DMF), while the undoped form of PANI is soluble in these organic solvents [30]. PANI has garnered significant attention due to its conductive and antimicrobial properties [31]. The basic

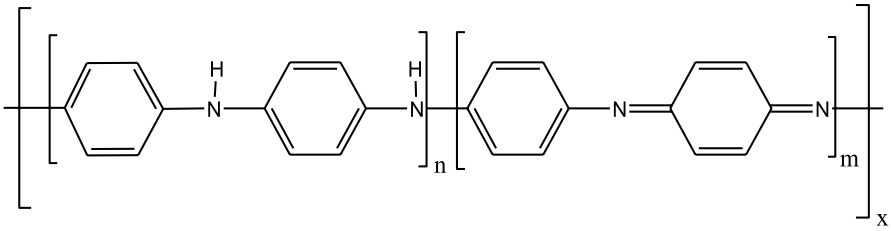

Fig. 1 Structure of polyaniline

structure of PANI is illustrated in Fig. 1, where the leucoemeraldine state is composed of the benzenoid state, with the H elements in proximity to the N elements. In contrast, the pernigraniline state is comprised of the quinonoid state, where no H element is attached to N elements. The redox state of PANI is dependent on the quantity of m and n present in the PANI chains.

Ideally, the *m*:*n* ratio for leucoemeraldine, pernigraniline, and incompletely oxidized emeraldine state should be 1:0, 0:1, and 1:1, respectively. However, the synthesis process and level of doping can cause variations in these ratios. While leucoemeraldine and pernigraniline are nonconductive, the moderately doped state known as emeraldine salt exhibits conductive behavior [32]. Therefore, it is essential to maintain a balance between the benzenoid and quinonoid groups in the emeraldine salt to achieve the desired electrochemical properties. Various redox structures of polyaniline, including leucoemeraldine, emeraldine, and pernigraniline in their base and salt forms, are illustrated in Fig. 2.

The use of quaternary ammonium chitosan-g-PANI results in a material that exhibits both conductivity and antibacterial properties while being biodegradable [33]. In another study, a copolymer of polyaniline and polypyrrole functionalized with chitosan was synthesized and used for Zn (II) adsorption and showed antimicrobial activity against *E. coli* and *E. agglomerans* bacteria [34]. Similarly, a polypyrrole-graft-chitosan copolymer was synthesized and compared with several antibiotics, showing equipotent activity with Erythromycin and Amikacin [35]. Other studies have also explored the antibacterial properties of polyaniline and its composites with various drugs, dyes, nanoparticles, and other materials. Kashyap et al. [36] synthesized polyaniline and its drug composites using an oxidative polymerization method with some drugs like trimethoprim, neomycin, and streptomycin. The authors used *S. aureus, B. subtilis, S. pyrogenes, S. mutant* (gram-positive bacteria), and *S. typhi, K. pneumoniae, E. coli, P. aeruginosa* (gram-negative bacteria) for antibacterial activity. The drug composites also showed antituberculosis activity in contradiction to *Mycobacterium tuberculosis* H_{37}RV.

Dye-substituted PANIs have shown antimicrobial behavior against various bacterial and fungal strains. Dyes such as methylene blue, malachite green, azure B, methyl violet, rhodamine 6G, and methyl orange have been used in the synthesis of dye-substituted polyanilines [37]. Furthermore, polyaniline and Fe_2O_3/PANI nanoparticles were synthesized and tested for antibacterial activity against gram-positive bacteria *S. aureus* and gram-negative bacteria *E. coli*, as well as fungal strains [38].

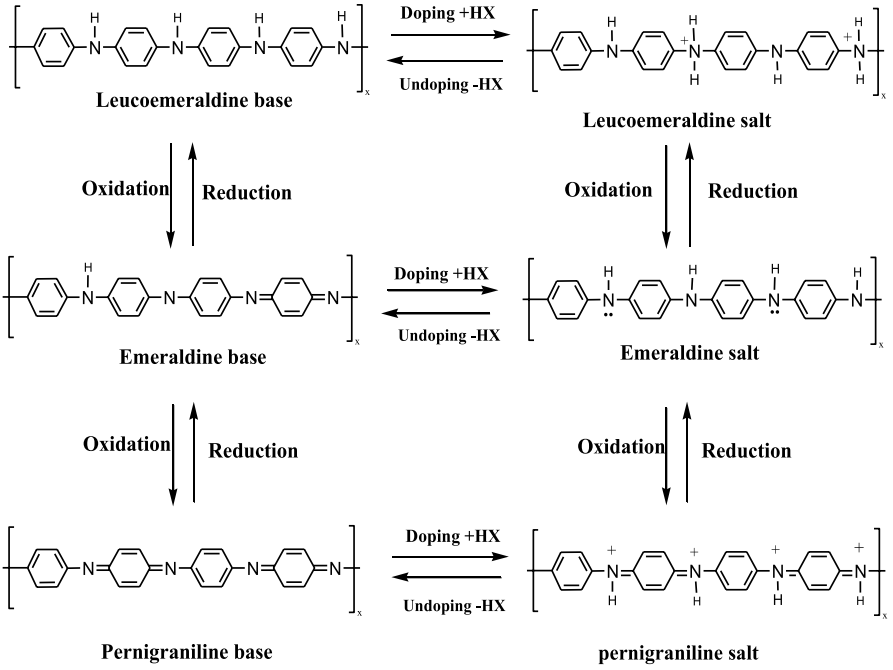

Fig. 2 Various redox structures of polyaniline

Usnic acid-doped polyaniline has been shown to possess bactericidal activity and anti-biofilm properties derived from lichens. Deposition of doped polyaniline on polyurethane foam may be a viable option for use as a wound dressing [39]. Additionally, a conducting nanocomposite of polypyrrole-co-polyindole doped with carboxylated CNT was synthesized to exhibit antioxidant, antibacterial, and thermal resistance properties [40].

Seyedaghazadeh et al. [41] synthesized an aniline-carbazole copolymer and its carbon-based nanocomposites using the oxidative polymerization technique, and studied their conductivity, antioxidant, and antibacterial properties. Rathore et al. [42] synthesized a chitosan–polyaniline–copper (II) oxide (Ch–PANI–CuO) nanocomposite for the removal of methyl orange dye, with maximum dye degradation of 94.6%. Pandiselvi and Thambidurai [43] synthesized a polyaniline ZnO/chitosan nanocomposite for the removal of reactive orange and methylene blue dyes, achieving removal efficiencies of 96% and 88.5%, respectively.

Functionalized dopants such as sulfonic acids have been used by many researchers to produce extra stable, soluble, and conductive polyaniline. Karaoglan and Bindal [44] synthesized pure PANI, PANI-BSA, PANI-HCl, and PANI-HCl-BSA polymers using the chemical oxidation polymerization technique. BSA doping provided both high conductivity and enhanced solubility. The conductivity of PANI-BSA, PANI-HCl-BSA, and PANI-HCl doped polymers was calculated as 1.39, 0.77, and 0.54 S cm^{-1}, respectively. Tong et al. [45] synthesized a photo-sensitive phytic acid (PAGA) by the ring opening reaction of glycidyl methacrylate and phytic acid

(PA), which was used to dope PANI. The doped PANI was then added to UV-curable resin to prepare a UV-curable polyaniline anticorrosive coating. Doping PANI with PAGA successfully increased the dispersion of PANI in coatings.

Yadav et al. [46] synthesized dodecyl benzene sulphonic acid (DBSA) doped PANI nanorods using a template-less route through in situ emulsion polymerization. The resulting sensor efficiently recognizes up to 1 ppm ammonia with good linearity in the 1–50 ppm range. Another method was employed to synthesize conductive PANI doped with dodecyl benzene sulfonic acid in xylene using chemical oxidative polymerization. The synthesized PANI solution was initially combined with UV improvable coating and then coated onto a polyethylene terephthalate (PET) sheet. The resulting UV coating/PANI conductive fused film on the PET sheet was flexible, clear, and had antistatic properties. This film can be useful as an antistatic product or biosensor [47].

Sulfonate zwitterionic ionic liquids were synthesized using methyl-imidazolium (mim.ZIL) or triphenylphosphonium (PPh3.ZIL) as the cations and were varied with dodecylbenzenesulfonic acid to be utilized as a co-doping agent for the synthesis of PANI through inverted emulsion polymerization method in toluene. This blend resulted in PANI with advanced DC conductivity values, and the improved response was achieved with mim.ZIL/DBSA in a molar ratio of 1.0, with DC equivalent to approximately 8 S cm^{-1}. These results are of significant importance for the development of novel electromagnetic shielding or absorbing resources [48].

Li et al. [49] synthesized polyaniline emeraldine-base form (PANI-EB) and polyaniline doped with dodecyl benzene sulfonic acid (PANI-DBSA) by chemical oxidation polymerization. Subsequently, polyaniline/acrylic resin coatings were primed using these polyaniline constituents as antifouling agents. The PANI coating displays good antifouling and anticorrosion activity. The parameters determined from a fit to the polarization plots demonstrate the beneficial role of PANI-DBSA in the anticorrosion performance of the acrylic resin coating.

Furthermore, the fluorophore polyaniline (PANI) was synthesized by doping with benzene sulfonic acid (BSA) to improve processability and mobility of p-electrons along with decreased p-stacking. BSA-PANI is utilized as a fluorophore to understand the interaction between BSA-PANI and commercial HEMs. The BSA-PANI can perform as a latent fluorophore [50]. Indoles play a crucial role in medicinal chemistry as they exhibit advanced biological activities and can produce novel biological properties when linked to other heterocyclic compounds. Indoles have been found to display potent antibacterial and antifungal activity against various test indicator strains, including Aspergillus niger ATCC 16404 [51].

Moreover, indole and its derivatives have been found to possess an extensive range of biological activities, such as anti-Alzheimer's disease, anti-inflammatory, anticancer, antihuman immunodeficiency virus, antibacterial, antidiabetic, antituberculosis, antioxidant, anti-coronavirus, and antifungal activities [52]. Aromatic heterocyclic compounds, which share similarities with various protein structures, are of great interest to organic and medicinal chemists. The rapid development of drug-resistant tuberculosis poses a significant challenge, necessitating the identification of new targets and medicinal candidates. Indole derivatives have emerged as promising antitubercular agents, with indole frameworks incorporating the new

non-covalent inhibitor 1,4-azaindole, which inhibits decaprenylphosphoryl-β-D-ribose2′-epimerase (DprE1), currently undergoing medical trials to treat Mycobacterium tuberculosis [53].

Chemical oxidative polymerization was employed to synthesize benzene sulfonic acid (BSA) doped polyaniline, using potassium persulfate ($K_2S_2O_8$) as an oxidant. To improve the processability and mobility of π-electrons, PANI was doped with benzene sulfonic acid (BSA). PANI copolymers were then synthesized, incorporating heterocyclic compound indole, which exhibits antimalarial, antibacterial, and antifungal activity.

The synthesized copolymers were subjected to characterization using various techniques, including FTIR, 1HNMR, GPC, and TGA. Antibacterial properties were studied against *E. coli* (MTCC 443), *P. aeruginosa* (MTCC 1688), *S. pyogenus* (MTCC 442), and *S. aureus* (MTCC 96), while antifungal properties were evaluated against *A. clavatus* (MTCC 1323), *A. niger* (MTCC 282), and *C. albicans* (MTCC 227). The antituberculosis activity was studied against Mycobacterium tuberculosis $H_{37}RV$, and the antimalarial property was evaluated against *Plasmodium falciparum*.

It was observed that the copolymers of polyaniline-indole exhibited superior biological activity compared to polyaniline alone. The synthesized copolymers demonstrated significant antibacterial, antifungal, antituberculosis, and antimalarial activity, making them potential candidates for use in various biomedical applications.

Experimental

Materials

Analytical grade reagents were utilized in the preparation of PANI and its copolymer. Merck, USA supplied aniline (for synthesis, $C_6H_5NH_2$, 99.5% pure) and benzene sulfonic acid (BSA, $C_6H_5O_3S$, 98% pure). Potassium persulfate (PPS, $K_2S_2O_8$) and ethanol (99.9% purity, containing 0.1% water) were purchased from Thomas Baker, India. Sigma-Aldrich, India supplied tetrahydrofuran (THF) and heterocyclic compound indole (C_8H_7N, 99% purity). All chemicals were used as received. Aniline and indole monomer ratios of 1:1, 1:2, and 2:1 were used.

Synthesis of polyaniline (PANI)

All chemicals utilized in the polyaniline synthesis process were of analytical grade and used as received. Polyaniline (PANI) was prepared through the chemical oxidative polymerization method. In this experiment, 6.3 mL of aniline was added to an aqueous acidic medium consisting of 1.0 M benzene sulfonic acid ($C_6H_6O_3S$, BSA) in 20 mL of water. BSA was used as a dopant. The resulting mixture was stirred in an ice bath at 0 °C until a homogeneous solution was obtained (at least 30 min). Polymerization was initiated by the slow dropwise addition of 1.0 M potassium persulfate ($K_2S_2O_8$, 80 mL) as an oxidant, under constant stirring at 0 °C. After 6 h, the completion of the polymerization reaction was confirmed, and the dark green

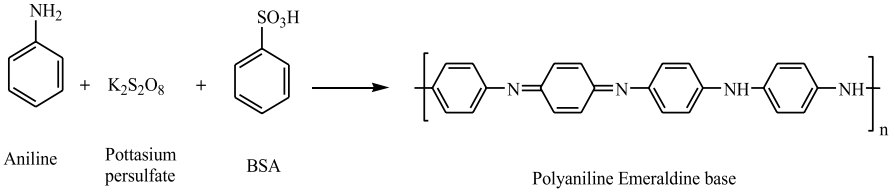

Scheme 1 Synthesis of polyaniline

emeraldine form of polyaniline (PANI) mixture was isolated through separation and washed continuously with distilled deionized water and ethanol until the filtrate was colorless, to ensure the complete removal of any impurities and unreacted reagents. The residue was oven-dried for 24 h at 50–60 °C to obtain a smooth powder of the polyaniline. The synthesized PANI was found to be in the dark green emeraldine salt form after washing, as shown in Scheme 1.

Synthesis of PANI-indole copolymers

The copolymer was synthesized via the chemical oxidation method using three different weight-to-volume ratios of aniline to indole (i.e., 1:1, 1:2, and 2:1). In a typical experiment, 1.6 mL of aniline and 1.6 g of indole were dissolved in an aqueous acidic medium containing 20 mL of 1.0 M benzene sulfonic acid ($C_6H_6O_3S$, BSA) while stirring in an ice bath at 0 °C. Next, 1.0 M potassium persulfate ($K_2S_2O_8$) was added dropwise to the acidified solution containing aniline at 0 °C under constant stirring to initiate polymerization. After 6 h, a dark green precipitate was obtained through filtration and washed with distilled deionized water and ethanol until the filtrate was colorless to ensure complete removal of any impurities and unreacted reagents. The pure PANI-indole copolymer synthesized using this method was found to be dark green in color after washing and drying. The residue was oven-dried for 24 h at 50–60 °C to obtain a free-flowing powder of the polyaniline-indole copolymer. Similarly, indole-to-aniline ratios of 1:2 and 2:1 were synthesized under the same experimental conditions. The reaction mechanism for the formation of the PANI-indole copolymers is shown in Scheme 2.

Characterization of synthesized copolymers

Chemical characterization is crucial to understanding the properties of polymeric materials and their structure. The synthesized PANI-indole copolymers were analyzed using several techniques, including FTIR, 1H-NMR, TGA, and GPC. The GPC method was utilized to determine the weight average molecular weight (Mw), number average molecular weight (Mn), and polydispersity index (PDI) of the copolymer composites using Perkin-Elmer 200 pumps and two ultra-Styragel columns.

ALPHA FTIR spectrometer (Bruker) was employed to obtain IR spectra between 400 and 4000 cm^{-1}. The chemical sample holder was flushed through dry air and

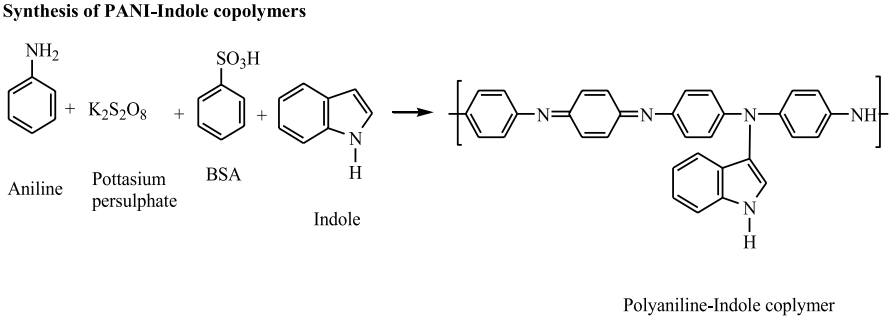

Scheme 2 Synthesis of polyaniline-indole copolymer

washed through a solvent for scanning the copolymers. For this spectral technique, dried samples were prepared with the KBr disk method.

The TGA thermal analysis method was used to determine the thermal properties of the synthesized copolymer. The thermal stabilities of the PANI-indole copolymers were investigated under a Nitrogen atmosphere using the TGA technique, from 25 to 800 °C at a heating rate of 10 °C/min.

The 1H-NMR spectra were obtained using the Advance NEO Spectrometer (Bruker) with a frequency of 1H-NMR of 500 MHz, and the solvent used was DMSO. The ^{1}HNMR and FTIR studies confirmed that doping caused structural changes in the polymer chains.

Results and discussion

The synthesis of PANI-indole copolymer using benzene sulfonic acid as a dopant and potassium persulfate as an oxidant was carried out in this study. To the best of our knowledge, this is the first time BSA has been used as a dopant in the synthesis of PANI-indole copolymer. The washing process effectively removed the oxidant from the copolymer, preventing contamination by the oxidation products of benzene sulfonic acid. The use of indole as an active heterocyclic compound in the synthesis of PANI copolymers was chosen due to its known biological activities, such as anticancer, antioxidant, anti-inflammatory, antifungal, anticholinesterase, and antibacterial properties [54]. Our aim was to synthesize a biologically active indole-based PANI copolymer to enhance the activity of PANI.

FTIR analysis

The FTIR spectra analysis confirmed that doping resulted in structural changes in the polymer chains. Table 1 and Fig. 3 present the FTIR data of both polyaniline and polyaniline-indole copolymer. Several shifted bands observed in the FTIR spectra of PANI-indole copolymer indicate an improvement compared to PANI alone. The FTIR spectra of the copolymer were obtained and compared with those of PANI

Table 1 FTIR spectra of PANI and PANI-indole copolymer

S. No.	Vibrational modes in copolymer chain	IR Frequency (cm^{-1})			
		PANI	PANI-indole copolymer (1:1)	PANI-indole copolymer (1:2)	PANI-indole copolymer (2:1)
	Para substituted	846	810	809	827
	Benzenoid rings	1164, 690	1159, 690	1154, 692	1158, 691
	Quinoid rings	1635	1570	1579	1567
	C–H stretching(aromatic ring)	2860	2987	2981	3050
	N–H stretching (PANI)	3265	3269	–	–
	N–H stretching (indole)	–	3417	–	–
	C–N stretching	1340	1311	1305	1303
	C–C stretching	1440	1384	1494	–
	C=C stretching (aromatic ring)	1635	1686	1652	–

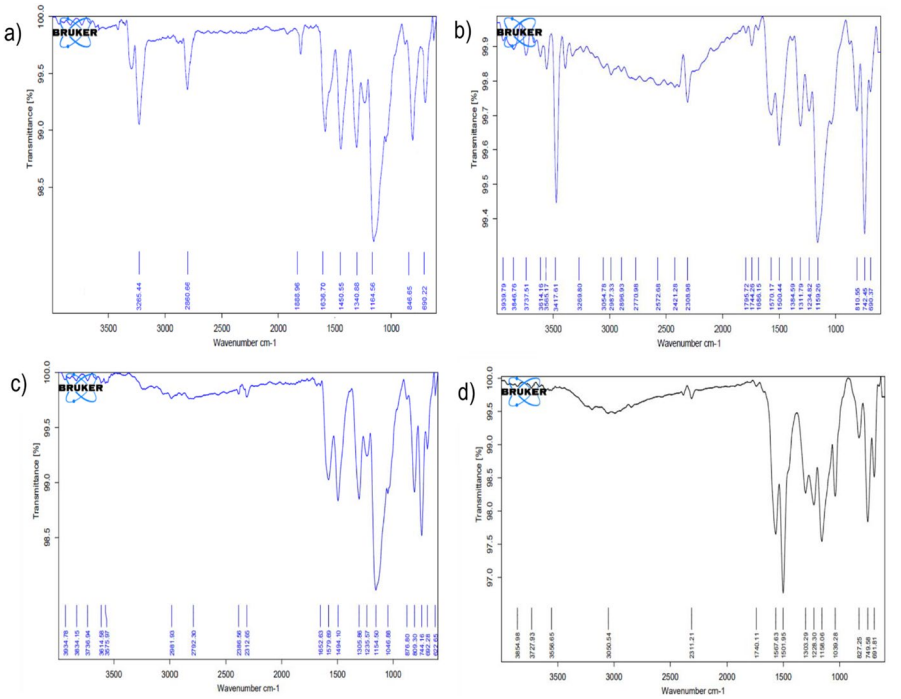

Fig. 3 IR spectra of (**a**) PANI, **b** PANI-indole copolymer [S1], **c** PANI-indole copolymer [S2], and **d** PANI-indole copolymer [S3]

alone. The specific peak of both polyaniline and indole is evident in the FTIR spectra of the copolymer as shown in Fig. 3, indicating the successful synthesis of the PANI-indole composite. The FTIR spectra of the synthesized copolymer containing indole and aniline were obtained in the range of 4000–600 cm^{-1}.

The band observed at 1570 cm^{-1} is attributed to the stretching vibrations of the N–H bond, indicating that indole did not polymerize through nitrogen. The characteristic peaks at 1500 cm^{-1} and 1686 cm^{-1} correspond to –C=C– stretching of pyrrole rings and benzene rings in indole, respectively, in the synthesized copolymer. The C–H stretching band is observed at 810 cm^{-1} and 690 cm^{-1} in the FTIR spectra of PANI-indole copolymer, and the peak at 742 cm^{-1} is the characteristic peak of the benzene ring in indole. The –C=C– bond presents equally in the N–B–N ring and N=Q=N ring. Here, B and Q are denoted as the benzenoid rings and the quinoid rings in the polyaniline chain structure. These results indicate that N–H bonds in indole are along the polymer backbone, suggesting that polymerization of indole and polyaniline occurred between carbon-3 of indole and the nitrogen atom of polyaniline. Comparison of the absorption wavenumbers reveals that some absorption wavenumbers of the copolymer are different from those of polyaniline.

^{1}H-NMR analysis

The NMR study was conducted to investigate the proton peaks in PANI and PANI-indole copolymer. The obtained 1H-NMR spectral data of polyaniline and PANI-indole copolymer are presented in Table 2 and Fig. 4. The wide-range multiplets observed in the range of 6.65–7.91 ppm correspond to the aromatic protons of the PANI polymer chain in the copolymer. The singlet peak at 5.8 ppm is attributed to the quinoid ring proton obtained in the polymer chain of the copolymer. Two singlet peaks in the range of 2.5–3.4 ppm are observed due to para-position N–H of PANI.

Furthermore, in the 1H NMR spectra of the N–H bond in indole, the peaks are observed at 10.5 ppm, whereas pyrrole peaks are observed in the range of 8.5–9.1 ppm. The combination of the benzene ring with the pyrrole ring led to the chemical shift of the N–H bond to move to a lower region of spectra. The chemical shift around 11–11.5 ppm can be assigned to the N–H bond in copolymers,

Table 2 ^{1}H-NMR data of PANI and PANI-indole copolymer

Name of compound	Chemical shift (ppm)	Observation
Polyaniline	6.71–7.95 (multiplet)	Aromatic protons
	5.6 (singlet)	Quinoid ring protons
	2.5–3.5 (singlet)	Due to –NH at the para position
Polyaniline-indole copolymer	6.65–7.91 (multiplet)	Aromatic protons
	5.8 (singlet)	Quinoid ring protons
	2.5–3.4 (singlet)	N–H at the para position of PANI
	10.5 (singlet)	N–H bond in indole
	11–11.5 (multiplet)	N–H bond present in the PANI-indole copolymer

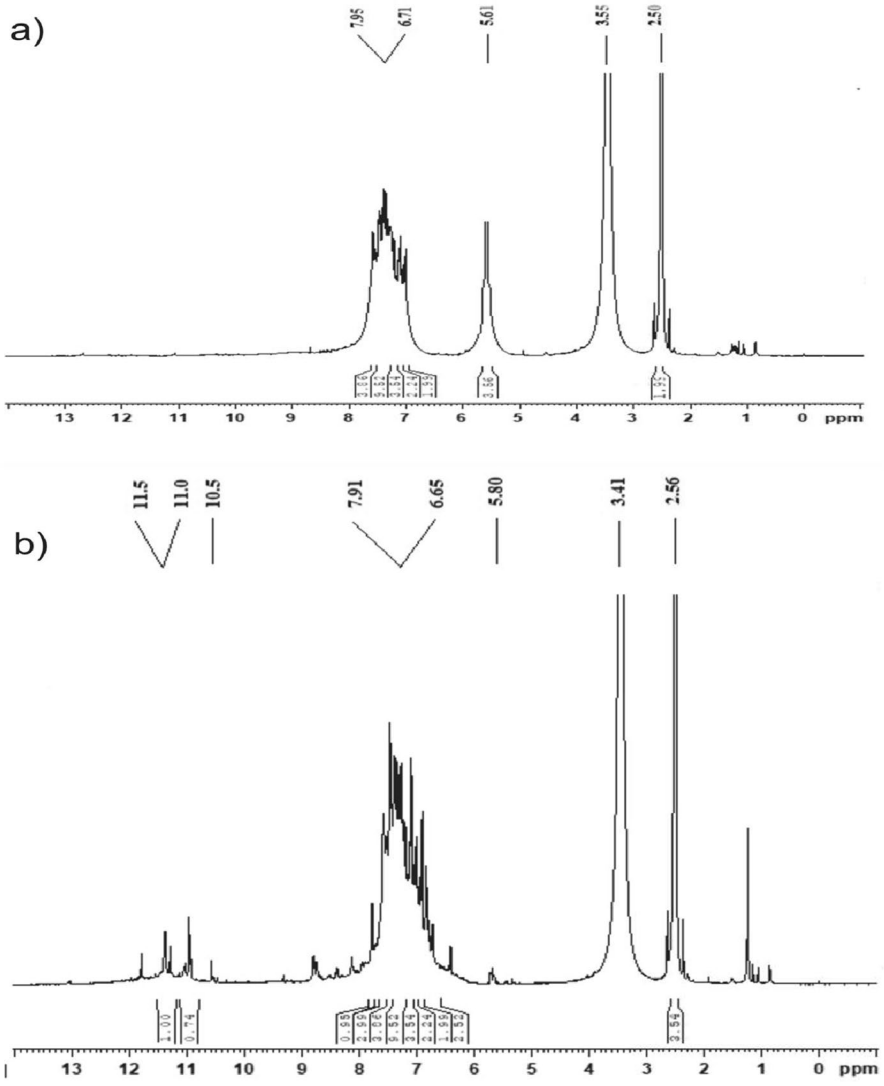

Fig. 4 ^{1}H-NMR data of (**a**) PANI and **b** PANI-indole copolymer

indicating that the N–H bond is present in the copolymer chain, which is consistent with the FTIR results.

Thermogravimetric analysis

The thermal properties of synthesized polymers are very essential for their applications. To confirm the copolymer formation and to compare the thermal behaviors of copolymers, TGA curve was obtained. The thermal stabilities of the PANI and

Table 3 Thermogravimetric analytical data of PANI and PANI-indole copolymer

Name of the composite	Weight losses at different temperatures (%)							
	100 °C	200 °C	300 °C	400 °C	500 °C	600 °C	700 °C	800 °C
PANI	96	95	84	78	76	52	50	48
PANI-indole copolymer (1:1)	99	95	90	81	72	61	57	54

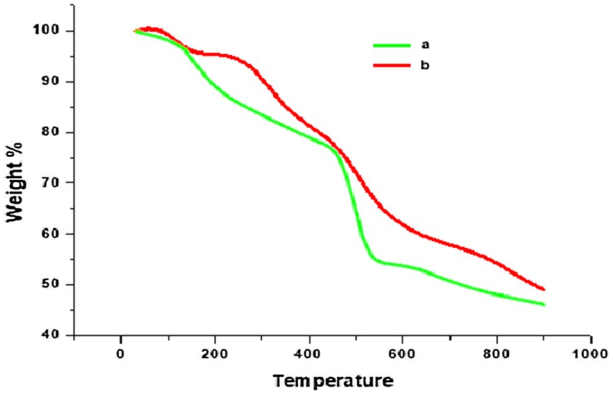

Fig. 5 TGA graph of (**a**) PANI and **b** PANI-indole copolymer [S1]

PANI-indole copolymer were examined by the TGA technique shown in Table 3 and Fig. 5. The weight loss temperatures of the synthesized PANI and its indole copolymers are different from each other. The primary weight loss of the copolymer took place at below 100 °C, which could be ascribed to exclusion of lightly bonded H_2O molecules present in the copolymer, while the weight losses observed below 250 °C may have stemmed from the loss of dopants. Both PANI and PANI-indole copolymer were prepared by the same doping agent that's why both are showed weight losses below 250 °C. The weight loss observed above 500 °C resulted from the degradation of the PANI-indole copolymer. The consequent weight loss is related to the continuing breakdown of the PANI-indole copolymer. The graph identifies that PANI-indole copolymer is more thermal stable as compared to PANI individuals. Additionally, the indole heterocyclic compound molecules rise the inflexibility of polymer chains of the synthesized copolymers. Thermal behaviors also support that synthesized polymer is indole containing polymer.

The thermal properties of polymers are critical for their practical applications. In order to confirm the copolymer formation and compare the thermal properties of the copolymers, TGA analysis was conducted. The TGA curves for PANI and PANI-indole copolymer are presented in Table 3 and Fig. 5. The weight loss temperatures of the synthesized PANI and its indole copolymers are distinguishable from each other. The initial weight loss of the copolymer occurred at below 100 °C, which could be attributed to the removal of loosely bonded H_2O molecules present in the copolymer, while the weight losses observed below 250 °C may have resulted

from the loss of dopants. Since both PANI and PANI-indole copolymer were prepared using the same doping agent, they showed weight losses below 250 °C. The weight loss observed above 500 °C was due to the degradation of the PANI-indole copolymer. The subsequent weight loss is related to the ongoing breakdown of the PANI-indole copolymer. The TGA data indicates that the PANI-indole copolymer is more thermally stable than PANI alone. Additionally, the incorporation of indole heterocyclic compound molecules enhances the rigidity of the polymer chains in the synthesized copolymers. The thermal behavior data supports the presence of indole in the copolymer.

Gel permeation chromatography

The molecular weight and polydispersity index (PDI) of PANI and PANI-indole copolymers play a crucial role in determining their properties and potential applications. Gel permeation chromatography (GPC) was used to determine these parameters. The GPC analysis revealed that the PANI-indole copolymers exhibited only a single peak, indicating the successful incorporation of indole moieties into the PANI backbone. This result also indicates that any unreacted aniline and indole moieties were effectively removed by washing with deionized distilled water and ethanol.

The polydispersity index (PDI) values for PANI and PANI-indole copolymers with different ratios of aniline to indole (1:1, 1:2, and 2:1) were determined from the GPC data. The PDI values were found to be 1.53, 1.13, and 1.532, respectively, indicating that the PANI-indole copolymers have a narrower molecular weight distribution than PANI alone. These results suggest that the incorporation of indole moieties into PANI leads to more homogeneous polymerization, resulting in a more uniform product with enhanced properties. The GPC results are summarized in Table 4.

Biological activity

Antimicrobial properties

The antibacterial and antifungal activity of PANI-indole copolymer was evaluated against four different bacterial cultures and three fungal cultures, using the micro broth dilution method at various concentrations (200, 100, 50, 25, 12.5,

Table 4 GPC data of polyanilne and polyaniline-indole copolymers

S. No.	Name of the copolymers	M_w (g/mol)	M_n (g/mol)	PDI (M_w/M_n)
1	PANI	1846	1515	1.21
2	PANI-indole copolymer 1:1 (S1)	4945	3232	1.53
3	PANI-indole copolymer 1:2 (S2)	1690	1494	1.13
4	PANI-indole copolymer 2:1 (S3)	3641	2375	1.532

Table 5 Antibacterial activity of PANI, PANI-indole copolymer, and some standard drugs

Minimal inhibition concentration (MIC) [μg/mL]						Reference
Sr. No.	Name of composite/standard drugs	*E. coli* (MTCC 443)	*P. aeruginosa* (MTCC 1688)	*S. aureus* (MTCC 96)	*S. pyogenus* (MTCC 442)	
1	PANI-indole copolymer (S1)	62.5	50	100	25	
2	PANI	475	95	120	120	[36]
3	Ampicillin	32	–	40	25	
4	Chloramphenicol	50	50	50	50	
5	Ciprofloxacin	25	25	50	50	
6	Norfloxacin	10	10	10	10	

Table 6 Antifungal activity of PANI, PANI-indole copolymer, and some standard drugs

Minimal fungicidal concentration [μg/mL]					Reference
Sr. No.	Name of composite/standard drugs	*C. albicans* (MTCC 227)	*A. niger* (MTCC 282)	*A. clavatus* (MTCC 1323)	
1	PANI-indole copolymer (S1)	**250**	500	250	
2	PANI	500	250	250	[37]
3	Nystatin	100	100	100	
4	Greseofulvin	500	100	100	

and 6.250 μg/mL). The bacterial cultures included two gram-negative bacteria (*P. aeruginosa* (MTCC 1688) and *E. coli* (MTCC 443)) and two gram-positive bacteria (*S. pyogenus* (MTCC 442) and *S. aureus* (MTCC 96)), while the fungal cultures consisted of *A. niger* (MTCC 282), *A. clavatus* (MTCC 1323), and *C. albicans* (MTCC 227). The minimum inhibitory concentration (MIC) was used to assess the antibacterial and antifungal activities of PANI and PANI-indole copolymer, with MIC being defined as the lowest level of antibiotics in a culture medium that can prevent bacterial or fungal growth. The zone of inhibition, which refers to the area around an antibiotic disk with no bacterial growth, was also determined.

The antibacterial and antifungal activities of PANI and PANI-indole copolymer are presented in Tables 5 and 6 and Figs. 6 and 7, respectively. The synthesized PANI-indole copolymer showed better antibacterial and antifungal activity than PANI. The antibacterial activity of PANI-indole copolymer was also compared with that of other standard drugs, including ampicillin, chloramphenicol, norfloxacin, gentamycin, and ciprofloxacin. The results indicate that the PANI-indole copolymer has promising potential as a prophylactic agent against bacterial and fungal infections.

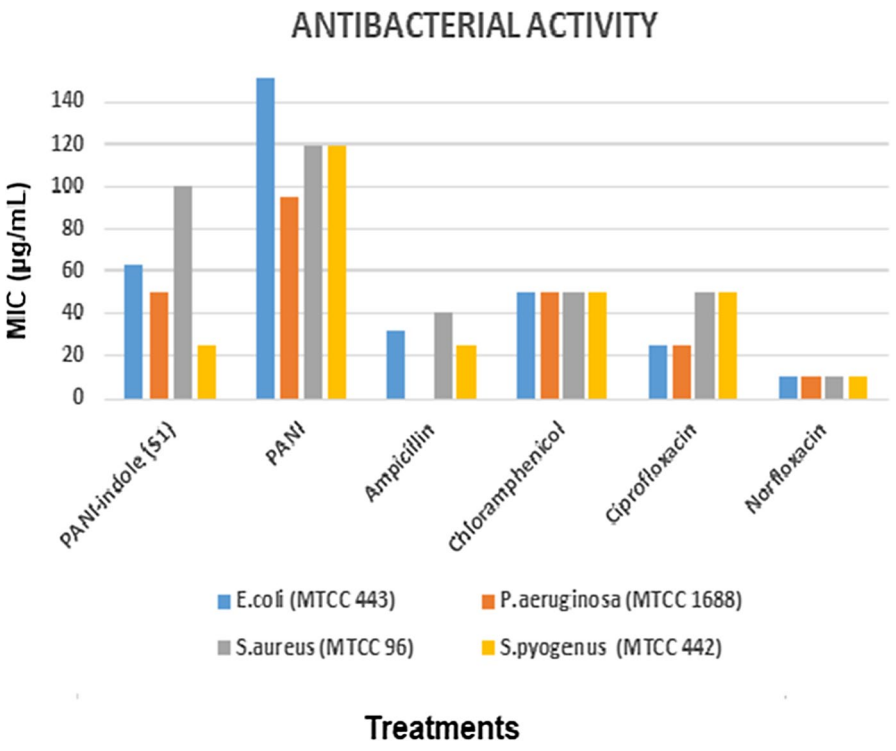

Fig. 6 Antibacterial activity of PANI, PANI-indole copolymer, and some standard drugs

Antituberculosis properties

The antituberculosis activity of PANI and PANI-indole copolymer (S1) was investigated against M. tuberculosis $H_{37}RV$ (acid fast bacilli, AFB) at various concentrations (100, 50, 12.5, 6.25. 3.125, 10, 5, 2.5, 1.25, 8, 4, 2, 1, 0.5, and 0.25 µg/mL). The minimum inhibition concentration (MIC) of PANI and PANI-indole copolymer against M. tuberculosis $H_{37}RV$ is summarized in Table 7. Tuberculosis is an infectious disease caused by the gram-positive bacteria M. tuberculosis, which primarily attacks the lungs but can also damage other parts of the body [55]. The polyaniline-indole copolymer can potentially target the cell wall synthesis of M. tuberculosis, thereby inhibiting the growth of the bacteria. These findings suggest that PANI-indole copolymer has the potential to be used as a therapeutic agent against tuberculosis, and further investigations are needed to explore its efficacy in treating this disease.

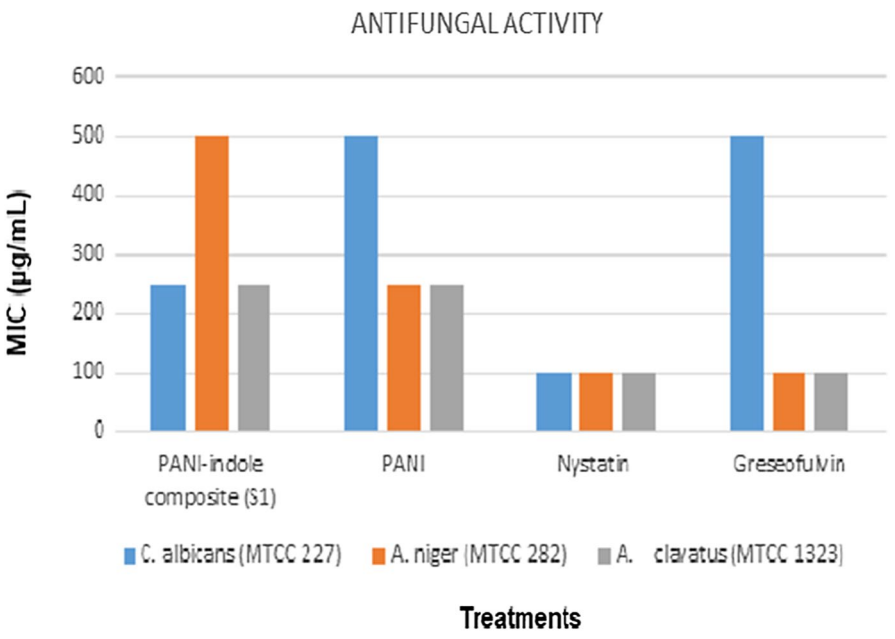

Fig. 7 Antifungal activity of PANI, PANI-indole copolymer, and some standard drugs

Table 7 The antituberculosis activity of PANI, PANI-indole copolymer, and some standard drugs

Antituberculosis activity			
Method: Lowenstein–Jensen medium [conventional method]			
Bacteria: $H_{37}RV$			
Sr. No.	Name of composites/standard drugs	MIC µg/ml	Reference
1	PANI-indole copolymer (S1)	1.25 µg/ml	
2	PANI	2.5 µg/ml	[36]
3	Isoniazid	0.20 µg/ml	
4	Rifampicin	0.25 µg/ml	

Table 8 Antimalarial activity of PANI-indole copolymer, and standard drugs

Antimalarial activity [*Plasmodium falciparum*] Minimal inhibition concentration		
Sr.No.	Name of composite/standard drugs	Mean IC50 values
1	PANI-indole copolymer (S1)	0.56 µg/mL
2	Chloroquine	0.020 µg/mL
3	Quinine	0.268 µg/mL

Antimalarial activity

The antimalarial activity of the PANI-indole copolymer (S1) was evaluated against *P. falciparum* parasites, as shown in Table 8. The *P. falciparum* strain was maintained in RPMI 1640 medium supplemented with 1% D-glucose, 25 mM HEPES, 0.23% sodium bicarbonate, and 10% heat-inactivated human serum. Asynchronous *P. falciparum* parasites in the ring phase were obtained by treatment with 5% D-sorbitol. A starting parasitemia of 0.8–1.5% at 3% hematocrit in a total volume of 200 µL RPMI 1640 medium was used for the assay, and parasitemia was determined using Jaswant Singh Bhattacharya (JSB) stain, which stains parasitized cells. The culture plates were incubated at 37 °C in a candle jar. For the assay, 5 mg/mL of the test samples were prepared in DMSO and subsequent dilutions were made using culture medium. The diluted samples (20 µL) were added to the test wells to obtain final concentrations ranging from 0.4 to 100 µg/mL in duplicate wells containing the parasitized cell preparation. After 36–40 h of growth, thin blood smears were prepared from each well and stained with JSB. The development of ring-phase parasites into trophozoites and schizonts in the presence of various concentrations of the experimental mediators was microscopically observed. The concentration of the test mediator that completely inhibited growth into schizonts was noted as the minimum inhibitory concentration (MIC) [56, 57]. The average number of rings, trophozoites, and schizonts per 100 parasites from identical wells were noted after 38 h of growth, and the percent growth inhibition relative to the control group was calculated. This data can help in assessing the potential use of PANI-indole copolymers in combination with other antimalarial agents as a prophylactic measure against malaria.

Conclusion

In conclusion, the successful synthesis of PANI-indole copolymer using the chemical oxidative polymerization method has been demonstrated. The copolymerization of aniline and indole was thoroughly characterized using various techniques such as FTIR, 1H-NMR, TGA, and GPC, revealing the properties of the copolymer to be strongly dependent on the ratios of monomer concentration. The synthesized copolymer exhibited excellent antibacterial activity against both gram-positive and gram-negative bacteria, outperforming PANI and standard drugs. Specifically, the PANI-indole copolymer demonstrated remarkable antimicrobial activity against *S. pyogenus* (MTCC 442) due to its excessive positive charge and oxidizing potential. Moreover, the copolymer also displayed good antituberculosis and antimalarial activity when compared to PANI. Thus, the PANI-indole copolymer shows potential as a material for decontamination of microbes. The findings suggest that by controlling the monomer concentrations in polymerization solutions, copolymers with desirable properties can be synthesized. Overall, this study provides valuable insights for the development of new materials with enhanced antimicrobial properties.

Acknowledgements The authors express their gratitude to SICART Vallabh Vidyangar and SAIF, Chandigarh for providing analytical and spectral data. Additionally, we extend our appreciation to Microcare Laboratory, Surat for conducting biological screening of the synthesized compounds. We would also like to acknowledge the Head, Department of Chemistry at UCoS, MLSU, Udaipur, Rajasthan for providing necessary laboratory facilities.C. Ameta sincerely acknowledges Ministry of Higher Education, Government of India and Ministry of Higher Education, Government of Rajasthan, India for providing NMR facility under RUSA 2.0, Research and Innovation project.

Funding This research did not receive any specific grant from funding agencies in the public, commercial, or not-for-profit sectors.

Declarations

Conflict of interest The authors declare no conflict of interest.

References

1. Maria L, Carrillo A, Verdugo AJ, Olivas A, Guerrero JM, De la Cruz EC, Ramirez NN (2019) Synthesis and novel purification process of PANI and PANI/AgNPs composite. Molecules 24:1621–1634. https://doi.org/10.3390/molecules24081621
2. Gao N, Yu J, Chen S, Xin X, Zang L (2021) Interfacial polymerization for controllable fabrication of nanostructured conducting polymers and their composites. Synth Met 273:116693–116707. https://doi.org/10.1016/j.synthmet.2020.116693
3. Ajabshir SZ, Morassaei MS, Niasari MS (2019) Eco-friendly synthesis of $Nd_2Sn_2O_7$–based nanostructure materials using grape juice as green fuel as photocatalyst for the degradation of erythrosine. Compos B 167:643–653. https://doi.org/10.1016/j.compositesb.2019.03.045
4. Rezayeenik M, Kamazani MM, Zinatloo-Ajabshir SZ (2023) $CeVO_4$/rGO nanocomposite: facile hydrothermal synthesis, characterization, and electrochemical hydrogen storage. Appl Phys A 129:47. https://doi.org/10.1007/s00339-022-06325-y
5. Esfahani MH, Ajabshir SZ, Naji H, Marjerrison CA, Greedan JE, Behzad M (2023) Structural characterization, phase analysis and electrochemical hydrogen storage studies on new pyrochlore $SmRETi_2O_7$ (RE = Dy, Ho, and Yb) microstructures. Ceram Int 49(1):253–263. https://doi.org/10.1016/j.ceramint.2022.08.338
6. Ajabshir SZ, Asil SAH, Niasari MS (2021) Simple and eco-friendly synthesis of recoverable zinc cobalt oxide-based ceramic nanostructure as high-performance photocatalyst for enhanced photocatalytic removal of organic contamination under solar light. Sep Purif Technol 267:118667. https://doi.org/10.1016/j.seppur.2021.118667
7. Hosseinzadeh G, Ghasemian N, Ajabshir SZ (2022) TiO_2/graphene nanocomposite supported on clinoptilolite nanoplate and its enhanced visible light photocatalytic activity. Inorg Chem Commun 136:109144. https://doi.org/10.1016/j.inoche.2021.109144
8. Etemadi H, Afsharkia S, Ajabshir SZ, Shokri E (2021) Effect of alumina nanoparticles on the antifouling properties of polycarbonate polyurethane blend ultrafiltration membrane for water treatment. Polym Eng Sci 25764:1–12. https://doi.org/10.1002/pen.25764
9. Ajabshir SZ, Ghasemian N, Kamazani MM, Niasari MS (2021) Effect of zirconia on improving NOx reduction efficiency of $Nd_2Zr_2O_7$ nanostructure fabricated by a new, facile and green sonochemical approach. Ultrason Sonochem 71:105376–105386. https://doi.org/10.1016/j.ultsonch.2020.105376
10. Ajabshir SZ, Morassaei MS, Amiri O, Niasari MS (2019) Green synthesis of dysprosium stannate nanoparticles using Ficus carica extract as photocatalyst for the degradation of organic pollutants under visible irradiation. Ceram Int. https://doi.org/10.1016/j.ceramint.2019.11.072
11. Mahdavi K, Ajabshir SZ, Yousif QA, Niasari MS (2022) Enhanced photocatalytic degradation of toxic contaminants using Dy_2O_3-SiO_2 ceramic nanostructured materials fabricated by a new, simple and rapid sonochemical approach. Ultrason Sonochem 82:105892. https://doi.org/10.1016/j.ultsonch.2021.105892

12. Qazvini NT, Zinatloo S (2011) Synthesis and characterization of gelatin nanoparticles using CDI/NHS as a non-toxic cross-linking system. J Mater Sci Mater Med 22:63–69. https://doi.org/10.1007/s10856-010-4178-2
13. Ajabshir SZ, Qazvinia NT (2014) Inverse miniemulsion method for synthesis of gelatin nanoparticles in presence of CDI/NHS as a non-toxic cross-linking system. JNS 4:267–275
14. Bumaa B, Uyanga E, Sevjidsuren G, Davaasambuu J, Altantsog P (2021) Evolution of electrochemical properties of polyaniline doped by graphene oxide. Polym Bull. https://doi.org/10.1007/s00289-021-03837-0
15. Naghib S, Behzad F, Rahmanian M, Zare Y, Rhee K (2020) A highly sensitive biosensor based on methacrylated graphene oxide-grafted polyaniline for ascorbic acid determination. Nanotechnol Rev 9:760–767. https://doi.org/10.1515/ntrev-2020-0061
16. Popov A, Aukstakojyte R, Gaidukevic J, Lisyte V, Minkstimiene KA, Barkauskas J, Ramanaviciene A (2021) Reduced graphene oxide and polyaniline nanofibers nanocomposite for the development of an amperometric glucose biosensor. Sensors 21:948–963. https://doi.org/10.3390/s21030948
17. Chen C, Geo Y (2016) Electrochemical properties of poly(aniline-co-N-methylthionine) for zinc conducting polymer rechargeable batteries. Electrochim Acta 190:240–247. https://doi.org/10.1016/j.electacta.2015.12.125
18. Chen C, Geo Y (2017) Electrosynthesis of poly(aniline-co-azure B) for aqueous rechargeable zinc-conducting polymer batteries. Electrochim Acta 252:226–234. https://doi.org/10.1016/j.electacta.2017.08.195
19. Hong X, Liu Y, Li Y, Wang X, Fu J, Wang X (2020) Application progress of polyaniline, polypyrrole and polythiophene in lithium-sulfur batteries. Polymers 12:331–358. https://doi.org/10.3390/polym12020331
20. Yu Z, Li J, Bade SGR (2017) Single-layer Universal high work function flexible anode for simplified ITO-free organic and perovskite light-emitting diodes with ultra-high efficiency. Asia Mater 9:411–419. https://doi.org/10.1038/am.2017.108
21. Celiesiute R, Ramanaviciene A, Gicevicius M, Ramanavicius A (2018) Electrochromic sensors based on conducting polymers, metal oxides, and coordination complexes. Crit Rev Anal Chem 49:195–208. https://doi.org/10.1080/10408347.2018.1499009
22. Zhang L, Wang B, Li X, Xu G, Dou S, Zhang X, Chen X (2019) Further understanding of the mechanisms of electrochromic devices with variable infrared emissivity based on polyaniline conducting polymers. J Mater Chem 32:9878–9891. https://doi.org/10.1039/C9TC02126D
23. Bryan AM, Santino LM, Lu Y, Acharya S, D'Arcy JM (2016) Conducting polymers for pseudocapacitive energy storage. Chem Mater 28:5989–5998. https://doi.org/10.1021/acs.chemmater.6b01762
24. Jiang D, Murugadoss V, Wang Y, Lin J, Ding T, Qian W (2019) Electromagnetic interference shielding polymers and nanocomposites- a review. Polym Rev 59:280–337. https://doi.org/10.1080/15583724.2018.1546737
25. Pina DC, Ermelinda F (2022) Advances in polyaniline for biomedical applications. Curr Med Chem 29:329–357. https://doi.org/10.2174/0929867328666210419135519
26. Ibanez JG, Rincon ME, Granados SG, Chahma M, Quintero OAJ, Uribe BAF (2018) Conducting polymers in the fields of energy, environmental remediation, and chemical-chiral sensors. Chem Rev 118:4731–4816. https://doi.org/10.1021/acs.chemrev.7b00482
27. Babel V, Hiran BL (2021) A review on polyaniline composites: synthesis, characterization, and applications. Polym Compos 42:3142–3157. https://doi.org/10.1002/pc.26048
28. Itoi H, Hayashi S, Matsufusa H, Ohzawa Y (2017) Electrochemical synthesis of polyaniline in the micropores of activated carbon for high-performance electrochemical capacitors. Chem Commun 53:3201–3204. https://doi.org/10.1039/C6CC08822H
29. Bhandari S (2018) Polyaniline: structure and properties relationship. Polyaniline Blends Compos Nanocompos. https://doi.org/10.1016/B978-0-12-809551-5.00002-3
30. Zare EN, Abdollahi T, Motahari A (2018) Effect of functionalization of iron oxide nanoparticles on the physical properties of poly (aniline-co-pyrrole) based nanocomposites: experimental and theoretical studies. Arab J Chem 52:452–461
31. Makvandi P, Ali GW, Sala DF, Abdel-Fattah WI, Borzacchiello A (2019) Biosynthesis and characterization of antibacterial thermosensitive hydrogels based on corn silk extract, hyaluronic acid and nanosilver for potential wound healing. Carbohydr Polym 223:115023–115035. https://doi.org/10.1016/j.carbpol.2019.115023

32. Zhao X, Li P, Guo B, Ma PX (2015) Antibacterial and conductive injectable hydrogels based on quaternized chitosan-graft-polyaniline/oxidized dextran for tissue engineering. Acta Biomater 26:236–248. https://doi.org/10.1016/j.actbio.2015.08.006
33. Boeva ZA, Sergeyev VG (2014) Polyaniline: synthesis, properties, and application. Polym Sci 56:144–153. https://doi.org/10.1134/S1811238214010032
34. Kumar R, Oves MT, Al-Makishan NH, Barakat MA (2017) Hybrid chitosan/polyaniline-polypyrrole biomaterial for enhanced adsorption and antimicrobial activity. J Colloid Interface Sci 490:488–496. https://doi.org/10.1016/j.jcis.2016.11.082
35. Cabuka M, Alan Y, Yavuz M, Unal HI (2014) Synthesis, characterization, and antimicrobial activity of biodegradable conducting polypyrrole-graft-chitosan copolymer. Appl Surf Sci 318:168–175. https://doi.org/10.1016/j.apsusc.2014.02.180
36. Kashyap G, Ameta G, Ameta C, Ameta R, Punjabi PB (2019) Synthesis and characterization of polyaniline-drug conjugates as effective antituberculosis agents. Bioorg Med Chem Lett 29:1363–1369. https://doi.org/10.1016/j.bmcl.2019.03.040
37. Jangid NK, Chauhan NPS, Meghwal K, Ameta R, Punjabi PB (2015) Synthesis of dye- substituted polyanilines and study of their conducting and antimicrobial behavior. Cogent Chem 1:1084666–1084680. https://doi.org/10.1080/23312009.2015.1084666
38. Mohamed NI, Hassan SM, Khalil JK (2022) Preparation, characterization, and antimicrobial activity of polyaniline and Fe_2O_3/polyaniline composite nanoparticle. Iraq J Phys 20:48–56. https://doi.org/10.30723/ijp.v20i1.725
39. Santos MRD, Espinoza JJA, Costa MMD, Oliveira HPD (2018) Usnic acid-loaded polyaniline/polyurethane foam wound dressing: preparation and bactericidal activity. Mater Sci Eng C 89:33–40. https://doi.org/10.1016/j.msec.2018.03.019
40. Lakourj MM, Norouzian RS, Esfandyar M, Mir SG (2020) Conducting nanocomposites of polypyrrole-co-polyindole doped with carboxylated CNT: synthesis approach and anticorrosion/antibacterial/antioxidation property. Mater Sci Eng B 261:114673–114688. https://doi.org/10.1016/j.mseb.2020.114673
41. Seyedaghazadeh SF, Lakouraj MM, Hasantabar V (2018) Synthesis and characterization of poly (aniline-co-carbazole) conductive copolymer and its carbon-based nanocomposite. Iran Chem Congr 20
42. Rathore BS, Chauhan NPS, Rawal MK, Ameta SC, Ameta R (2020) Chitosan–polyaniline–copper(II) oxide hybrid composite for the removal of methyl orange dye. Polym Bull 77:4833–4850. https://doi.org/10.1007/s00289-019-02994-7
43. Pandiselvi K, Thambidurai S (2016) Synthesis of adsorption cum photocatalytic nature of polyaniline-ZnO/chitosan composite for removal of textile dyes. Desalin Water Treat 57:8343–8357. https://doi.org/10.1080/19443994.2015.1019365
44. Karaoğlan N, Bindal C (2018) Synthesis and optical characterization of benzene sulfonic acid doped polyaniline. Eng Sci Technol Int J 21(6):1152–1158. https://doi.org/10.1016/j.jestch.2018.09.010
45. Tong J, Pan W, Ma J, Luo J, Liu R (2023) Preparation of photosensitive phytic acid doped polyaniline and its application in UV-curable anticorrosive coatings. Prog Org Coat 175:107366. https://doi.org/10.1016/j.porgcoat.2022.107366
46. Yadav A, Kumar J, Shahabuddin M, Agarwal A, Saini P (2019) Improved ammonia sensing by solution processed dodecyl benzene sulfonic acid doped polyaniline nanorod networks. IEEE Access 7:139571–139579. https://doi.org/10.1109/ACCESS.2019.2942361
47. Chen CH, Wang JM, Chen WY (2020) Conductive polyaniline doped with dodecyl benzene sulfonic acid: synthesis, characterization, and antistatic application. Polymers 12:2970–2983. https://doi.org/10.3390/polym12122970
48. Soares BG, Nascimento MRS, Sena AS, Indrusiak T, Souto LFC, Pontes K (2020) Polyaniline co-doped with dodecyl benzene sulfonic acid and zwitterionic based ionic liquids prepared by inverse emulsion polymerization. Synth Met 266:116435–116440. https://doi.org/10.1016/j.synthmet.2020.116435
49. Li J, Bi J, Wang X, Wang H, Huang X, Li Y, Wang G (2022) Antifouling and anticorrosion properties of coatings based on polyaniline doped with dodecyl benzene sulfonic acid. Int J Electrochem Sci 17:22039. https://doi.org/10.20964/2022.03.10
50. Ture SA, Pattathil SD, Patil VB, Yelamaggad CV, Manez RM, Abbaraju V (2022) Synthesis and fluorescence sensing of energetic materials using benzenesulfonic acid-doped polyaniline. J Mater Sci Mater Electron 33:8551–8565. https://doi.org/10.1007/s10854-021-065377

51. Konus M, Çetin D, Kızılkan ND, Yılmaz C, Fidan C, Algso M, Kavak E, Kivrak A, Kızıldgan AK, Otur C, Mutlu D, Abdelsalam AH, Arslan S (2022) Synthesis and biological activity of new indole based derivatives as potent anticancer, antioxidant and antimicrobial agents. J Mol Struct 1263:133168. https://doi.org/10.1016/j.molstruc.2022.133168
52. Tianze L, Hui X (2022) Recent progress of bioactivities, mechanisms of action, total synthesis, structural modifications and structure-activity relationships of indole derivatives: a review. Mini Rev Med Chem 22:2702–2725. https://doi.org/10.2174/1389557522666220330123538
53. Bajad NG, Singh SK, Singh SK, Singh TD, Singh M (2022) Indole: A promising scaffold for the discovery and development of potential anti-tubercular agents. Curr Res Pharmacol Drug Discov 3:100119–100133. https://doi.org/10.1016/j.crphar.2022.100119
54. Hayallah ME, Kovacic AM et al (2022) Recent progress in biologically active indole hybrids: a mini review. Pharmacol Rep 74:570–582. https://doi.org/10.1007/s43440-022-00370-3
55. Kaplancikli ZA, Turan-Zitouni G, Chevallet P (2005) Synthesis and antituberculosis activity of new 3-alkylsulfanyl-1,2,4-triazole derivatives. J Enzym Inhib Med Chem 20:179–182. https://doi.org/10.1080/14756360500043471
56. Kaushik CP, Pahwa A (2018) Convenient synthesis, antimalarial and antimicrobial potential of thioethereal 1,4-disubstituted 1,2,3-triazoles with ester functionality. Med Chem Res 27:458–469. https://doi.org/10.1007/s00044-017-2072-x
57. Xu J, Hu F, Li S, Bao J, Yin Y, Ren Z, Deng Y, Tian F, Bao G, Liu J, Li Y, He X, Xi J, Lu F (2022) Fluorescent nitrogen-doped carbon dots for label live elder blood-stage *Plasmodium falciparum* through new permeability pathways. Molecules 27(13):4163–4174. https://doi.org/10.3390/molecules27134163

Publisher's Note Springer Nature remains neutral with regard to jurisdictional claims in published maps and institutional affiliations.

Springer Nature or its licensor (e.g. a society or other partner) holds exclusive rights to this article under a publishing agreement with the author(s) or other rightsholder(s); author self-archiving of the accepted manuscript version of this article is solely governed by the terms of such publishing agreement and applicable law.